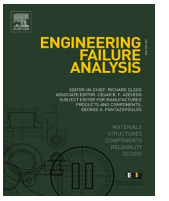
Engineering Failure Analysis 140 (2022) 106557



Contents lists available at ScienceDirect

Engineering Failure Analysis

journal homepage: www.elsevier.com/locate/engfailanal





Experimental and numerical investigation of heave damper hydraulic seal for racing car

Michel Azar [a], Marzio Grasso [a,*], Timothy Rose [a], Owen Carless [b], Chris StLeger-Harris [c], Carl Lawson [c]

[a] School of Aerospace, Transport and Manufacturing, Cranfield University, MK43 0AL, UK
[b] Red Bull Powertrains, Bradbourne Drive Tilbrook, Milton Keynes MK7 8BJ, UK
[c] Red Bull Technology, Bradbourne Drive Tilbrook, Milton Keynes MK7 8BJ, UK

ARTICLE INFO

Keywords:
Heave damper
Rubber seal
PTFE
Press-fit
High-pressure fluid

ABSTRACT

This article presents a combined experimental and numerical approach to analyse the failure of a heave damper hydraulic seal for racing car. The *post-mortem* analysis of the damaged seals was carried out with both optical microscopy and finite element analysis using material test data from Dynamic Modulus Analyser (DMA). The stress in the seal and damper was simulated modelling each step including the press-fitting on the piston, the interference with the cylinder and the oil pressure due to the service. The combination of the evidence collected from the numerical simulation and the observation of the surface damages on the seals proved that the cause of failure was the insufficient lubrication during high frequency, short stroke applications since these working conditions induce oil film break. The detailed damage mechanisms have been identified and explained and an alternative seal design that requires further study and testing in this application has been proposed.

1. Introduction

Elastomer and plastic seals can be found in a wide range of applications and industries such as aerospace, oil and gas and automotive. Seals degradation often leads to catastrophic failure, and they are crucial element of a reliable design. However, due to the hyperelastic behaviour of rubber, it is a challenging task to model the stress and strain level attained and predict the failure conditions. Moreover, applications characterised by high pressures and demanding dynamic conditions often use multicomponent seals and triangular shaped elastomer wedged between two triangular shaped back-up rings. Design and development of seals has mostly relied on empirical approaches rather than theoretical framework [1] that fail to accurately describe the complex response of the hyperelastic material and the multicomponent system.

Mechanical testing of reciprocating hydraulic seals has been a subject of study since 1935. As early as 1947 White, C. M. and Denny, D. F. observed the phenomenon of mixed lubrication at low speed and full hydrodynamic lubrication at higher speeds [2]. A study by Yoshimura et al. later supported this result using interferometry [3]. In the 1970 s Hirano and Kaneta [4] performed a series of tests on elastomer D-rings to study friction and sealing and observed a now well accepted phenomenon of rubber stiction at start-up and motion reversal due to the collapse of the fluid film. In this study the stability of a hydrodynamic film was related to the stroke length to contact

* Corresponding author.
E-mail address: marzio.grasso@cranfield.ac.uk (M. Grasso).

https://doi.org/10.1016/j.engfailanal.2022.106557
Received 28 February 2022; Received in revised form 13 June 2022; Accepted 15 June 2022
Available online 18 June 2022
1350-6307/© 2022 The Authors. Published by Elsevier Ltd. This is an open access article under the CC BY license (http://creativecommons.org/licenses/by/4.0/).

width ratio. It was found that a minimum ratio of 2:1 was required for a stable fluid film [5]. In two independent studies Rana and Sayles [6], and Bhaumik et al [5] built a reciprocating pressurized rig with the purpose of studying seal friction, leakage, and seal wear of reciprocating hydraulic seals [78]. The rig developed by Rana and Sayles [6] provided real-time data for hydraulic film, cavitation, debris accumulation, and seal wear but was limited to square section rod seals, and pressures up to 7 MPa. On the other hand, the rig developed by Bhaumik et al [5] was capable of pressures of up to 20 MPa but was also limited to square and U seals and incapable of gathering real-time seal wear data. Cheng et al [9] used physical performance tests paired with macro and micro analysis using high-definition microscope and scanning electron microscope images to identify failure in airplane actuator seals and suggest design improvements.

Theoretical modelling of elastomer seals has been largely hindered due to several factors such as their load–frequency dependent response, stress softening in cyclic loading, hysteresis, and stick–slip behaviour. In a series of papers, K. Nikas developed several numerical models to predict the electrohydrodynamic and mechanics of rectangular elastomeric seals [10–13]. These models also considered the effects of seal extrusion, transient response, the inclusion of a back-up ring on a low-pressure side, and a tandem seal configuration. K Nikas also develops a numerical model to study the deformation and contact pressure of a U seal [14]. Other approaches have used two-dimensional finite element analysis to solve initial static deflection and contact pressure coupled with Reynolds equation to evaluate dynamic film thickness, leakage, and contact pressures [15].

The most common failure mechanisms for dynamic hydraulic elastomer seals include abrasion and excessive wear, spiral twisting, extrusion, and thermal degradation. (see for example the work of Filtney R. [15] and System Seals and Parker Seals [16]). Excessive wear is typically caused by insufficient lubrication or contamination. Spiral twisting involves the twisting of the seal within its seat causing significant damage that can be avoided by using back-up rings or a harder grade material. Elastomers experience two kinds of extrusion failure: nibbled extrusion and single flash extrusion. The former is caused by repetitive small amount of extrusion while the latter consists of a single evident extrusion. Lastly, thermal degradation can occur at elevated temperatures and consists of cracks or striations on the surface of the seal.

Most of the approaches reported in the literature provide either empirical based description of the failure mechanisms of rubber seals or theoretical models that are limited to simple geometries (rectangular or circular). In the present work a combined empirical and theoretical model is presented and discussed to understand failure mechanisms of a multicomponent seal with a complex shape to identify the causes the sequence of failure and support possible design improvement.

2. The sealing system

The seal considered in this study is the Turcon® Wedgpak® II developed by Trelleborg Sealing Solutions [16]. The seal consists of a fluorocarbon elastomer wedged between two delta-shaped PTFE back-up rings. The backup rings are split diagonally to allow tangential variation in length for the assembly (1). The seal is press-fitted on the piston before the damper is assembled. The seal is then subjected to service loading under a high-pressure acting on one face of the back-up ring and atmospheric pressure on the opposite one. The different pressure acting on the two faces of the seal is responsible for further deformation of the seal (see Fig. 1).

The damper assembly consists mainly of a cylinder body, and a reciprocating piston. The seal is seated onto the piston as in Fig. 2 along with plastic bearings on either side to reduce friction and absorb side loads. The body is made of heat-treated Titanium 6Al-4 V while the piston is made of a steel alloy. Hydraulic fluid is used to create the pressure differential in the damper, and typically runs at 150C.

The Turcon® Wedgpak® II is designed for use both in static and light and dynamic applications such as aircraft utility actuators and landing gear shock absorbers. The seal can withstand pressures of up to 35 MPa and continuous reciprocating speeds of up to 3.0 m/s. The dynamic applications this seal is designed for are typically characterised by low frequency and high amplitude reciprocating motion with the seal exposed to long stroke and low frequency oscillations. However, when the component is adopted in racing cars the heave damper is also exposed to high frequency and short stroke oscillations.

3. Methods

A combined experimental and numerical approach was adopted to perform the failure analysis of the seal. The experimental approach consisted in the analysis of the failed seals under optical microscope and material characterisation of samples extracted from the seals while the numerical approach consisted in the identification of the stress and strain field experienced by each component using a 3D finite element model implemented in the commercial FEA package, ABAQUS. The steps are summarised in the flow chart shown in Fig. 3.

Failed seals have been analysed with microscopy to gather information on the type of damaged surfaces and identify the sequence



Fig. 1. PTFE Back-up ring with cut for assembly.

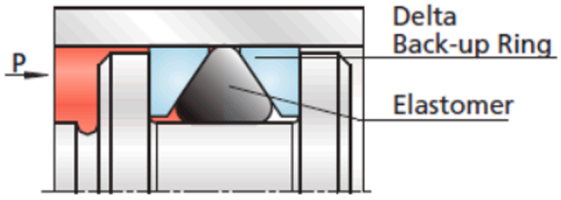


Fig. 2. Turcon® Wedgpak® II Seal [16].

of failure. The seal has experienced the extrusion of the back-up ring on the atmospheric pressure side and the unseating of the elastomer.

The identification of the failure sequence has been carried out comparing a seal affected by the failure in service with one new. New unused samples were collected as standalone seal packs whereas the failed samples consisted of damper piston and sealing components sub-assembly. Six sections with three damage conditions were defined on the piston (Fig. 4). The damage observed are back-up ring extrusion in section 2, 3 and 4; piston damage in sections 1 and 5; and no visible damage in section 6. 100X magnified pictures were taken of each section using a VHX-6000 Digital Microscope from Keyence Corporation. Stitching and automatic focusing features were used to achieve clear pictures. The images have been studied in detail to identify different failure mechanisms and the likely failure sequence.

The elastomer material characterisation was carried out with DMA whilst the stress–strain material response of the PTFE was based on data form literature [17]. A strain-controlled frequency sweep was conducted using a Q800 DMA from TA Instruments (Fig. 5). The test was run at two conditions corresponding to room temperature and 150 °C, this latter the temperature of the oil during service, the frequency ranging between 1 Hz and 20 Hz and a strain amplitude of 0.3%. Mooney-Rivlin, Neo-Hook, Odgen, and Polynomial hyperelastic models were compared in terms of goodness of fit of the material data. The best fitted model was implemented in the finite element (FE) model.

The heave damper was assumed axisymmetric and a 30° cut sector of the full damper geometry was used for the simulation in Abaqus. The model also incorporated a cut in the low-pressure backup ring, and the undeformed shape of the elastomer modelled using the cross-sectional image of a new seal extracted from the images taken during the optical microscopy. These details are essential to capture the effect of the back-up ring cut on the elastomer and estimate the initial contact pressures due to press-fitting.

The eight-node brick elements (C3D8I in the Abaqus library) [18] was used for the discretisation of the piston and body elements as this element provides an accurate estimation of the stress and strain field without significantly increase computation time. Specific element formulations are instead required for incompressible materials with high Poisson ratios such as PTFE and Fluorocarbon. The element formulations usually adopted are tetra4 (C3D4H in the Abaqus library) pyramid5 (C3D5H in the Abaqus library) and hex8 (C3D8H in the Abaqus library). The final model contains circa 88,000 nodes, 150,000 elements and 18 contacts (Fig. 6).

A cylindrical coordinate system has been used to define the boundary conditions. The two sets of surfaces on the sides of the sector model (1 in Fig. 7) were all constrained in the tangential direction to replicate the radial symmetry condition whilst surfaces 2 and 3 were constrained in the radial and vertical directions, respectively.

The 18 contacts defined to model the interactions of the different parts of the damper used different coefficient of friction taken from literature. A value of 0.04 was used for the contacts involving the PTFE, a value of 0.6 was used for the contact between the

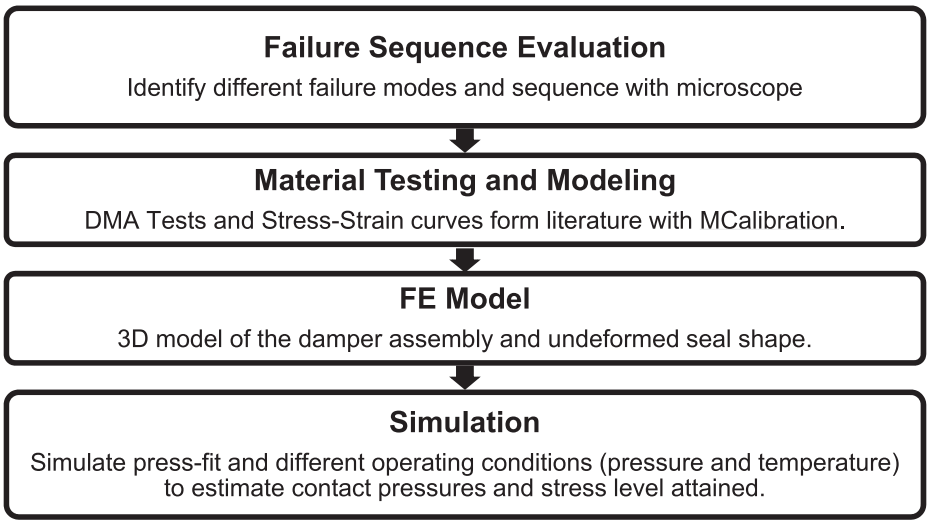


Fig. 3. Steps adopted in the methodology.

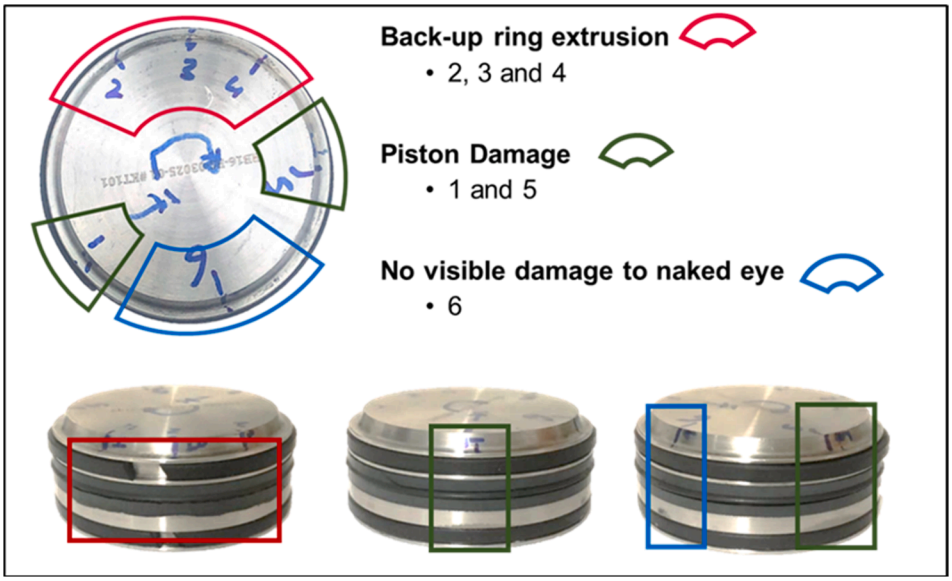


Fig. 4. Overview of sections of interest for on failed sample.



Fig. 5. TA Instruments Q800 DMA (left) and sample in tensile grips (right).

elastomer and metal components, and 0.17 was the coefficient of friction used between the piston and body [19 20].

The analysis has been implemented in three steps: interference fit to initialise the stresses due to the press-fit, temperature step to bring the system to the operating temperature and a pressure step to introduce the effect of the oil. In the pressure step a representative 20 MPa uniform pressure applied to the portion of the seal pack that is initially exposed to the high-pressure fluid, the edge of the high-pressure back-up ring (see Figs. 8 and 9).

3. Results

The three components of the seal (two back-up rings and the elastomer) are free to have relative movement as they can rotate on the piston about its axis. The first step was to check that the current relative position was the same relative position that the three components had when the damage in service developed. Across sections 3 to 4 in Fig. 4, wear marks on the elastomer were found to coincide with the abrasive marks and edge shape of the extruded low pressure back-up ring. In Fig. 10 taken from section 4, the red arrows highlight the aligned wear marks between the two components. Moreover, coincident light abrasive wear marks between the high- and low-pressure back-up rings like those shown in Fig. 11 from section 6 were found. The pictures show clear proof of minimal movement between the parts with light proof of alignment between the high- and low-pressure backup rings, and no evidence of alignment with the metal piston. For this reason, the minimum relative movement was only verified for the elastomer and back-up rings.

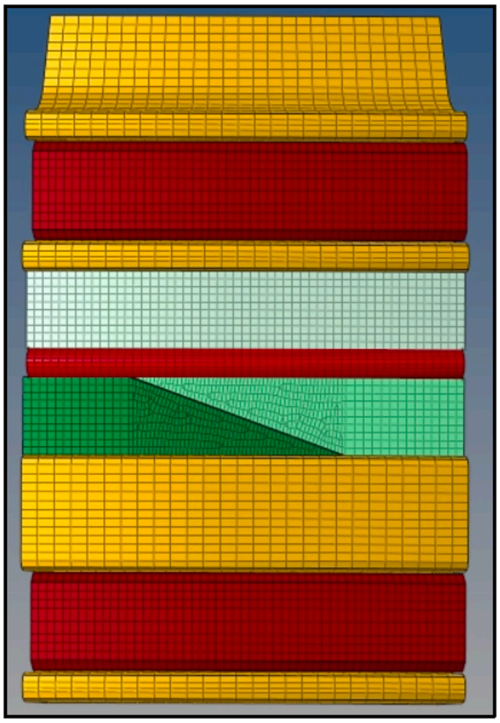


Fig. 6. Meshed piston and sealing components.

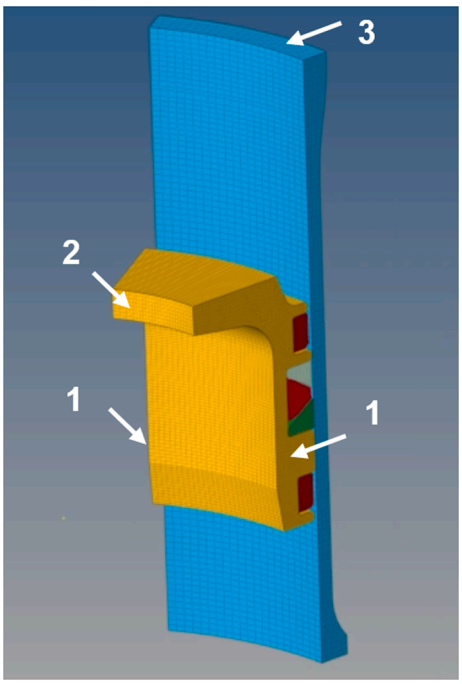


Fig. 7. Cut 30 FE Model.

It is assumed that the failure sequence can be described as the accumulation of damage in the elastomer followed by the extrusion of the low-pressure backup ring and elastomer unseating. For these reasons, the failure sequence is split into 5 steps summarised in Fig. 12. Each of the stages is described.

Typical run-in wear can be noticed when comparing the damaged and undamaged seal as shown in Fig. 13A taken from section 5.

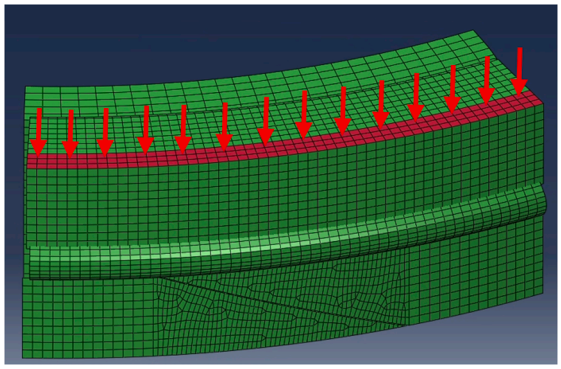


Fig. 8. Seal Pack: Region of uniform 20 MPa applied pressure.

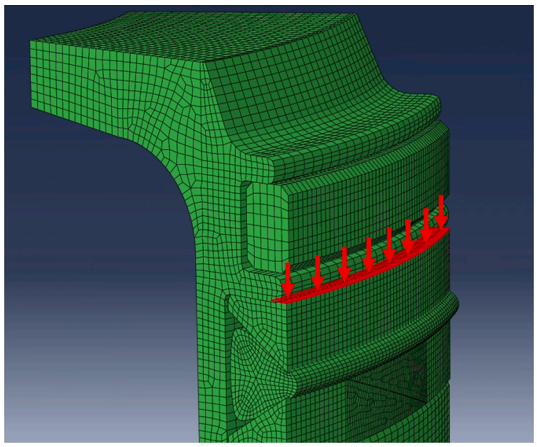


Fig. 9. Seal pack and piston assembly: Region of uniform 20 MPa applied pressure.

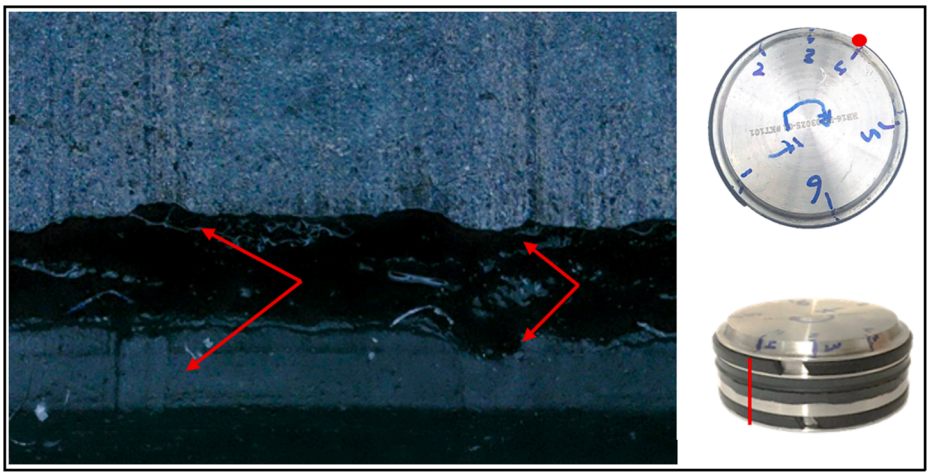


Fig. 10. Elastomer and low-pressure back-up ring wear alignment – section 4.

The flash line is worn away and the seal surface is visibly smoother. This is typical of seal behaviour during the run-in phase of operation [6]. However, in the other two sections around the seal circumferential thermal damage accumulation has occurred on the flash line as it can be seen in Fig. 13B taken from section 2.

Two forms of damage occur on the elastomer before the low-pressure back-up ring is extruded from the gap and they are nibbled extrusion and thermal degradation and are paired with light PTFE discolouration and wear [15].



Fig. 11. High- to low-pressure back-up ring wear alignment – section 6.

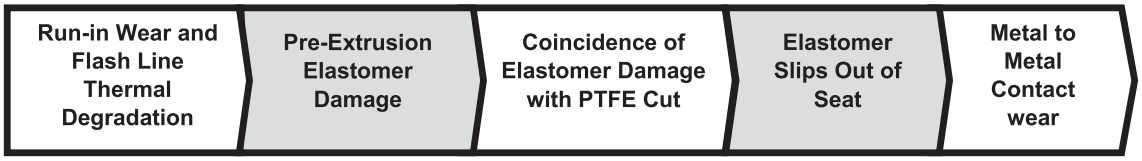


Fig. 12. 5-step failure sequence summary.

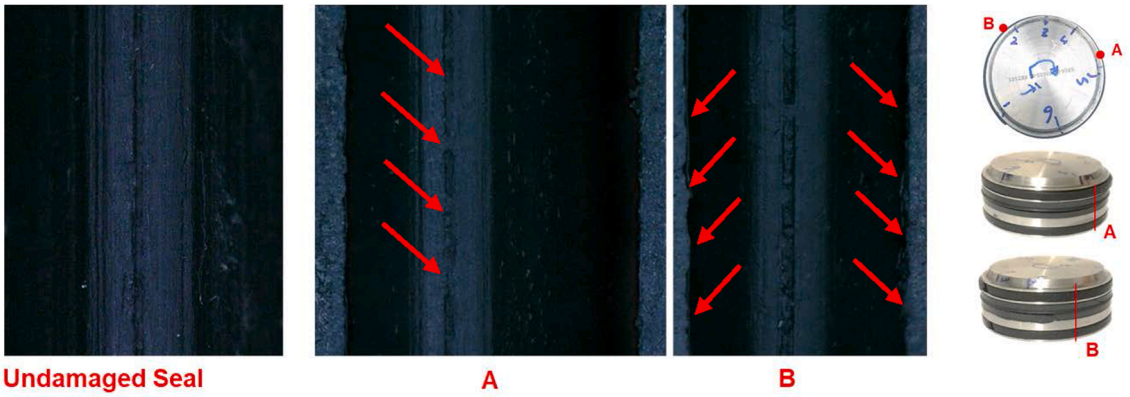


Fig. 13. Flash line wear and thermal degradation.

Nibbled extrusion is most notable in section 5 on the low-pressure side of the elastomer (Fig. 14 A). This damage is also paired with light PTFE discolouration. Nibbled extrusion was also found in sections 2, 3 and 4 as shown in Fig. 14B taken from section 2.

Nibbled extrusion was observed in section 5 where no PTFE extrusion has occurred as well as in other sections where the extrusion was observed that strongly suggested that the nibbled extrusion happened prior to the back-up ring extrusion.

Signs of thermal degradation are most notable in section 6. This damage is characterised by long diagonal striations on the surface of the seal, as highlighted by the red square in Fig. 15 A. This damage is also found from section 2 through to 4 where back-up ring extrusion occurs as shown in Fig. 15 B.

Like the nibbled extrusion, prevalence of this failure in sections without PTFE extrusion, it is assumed that thermal degradation occurs prior to back-up ring extrusion.

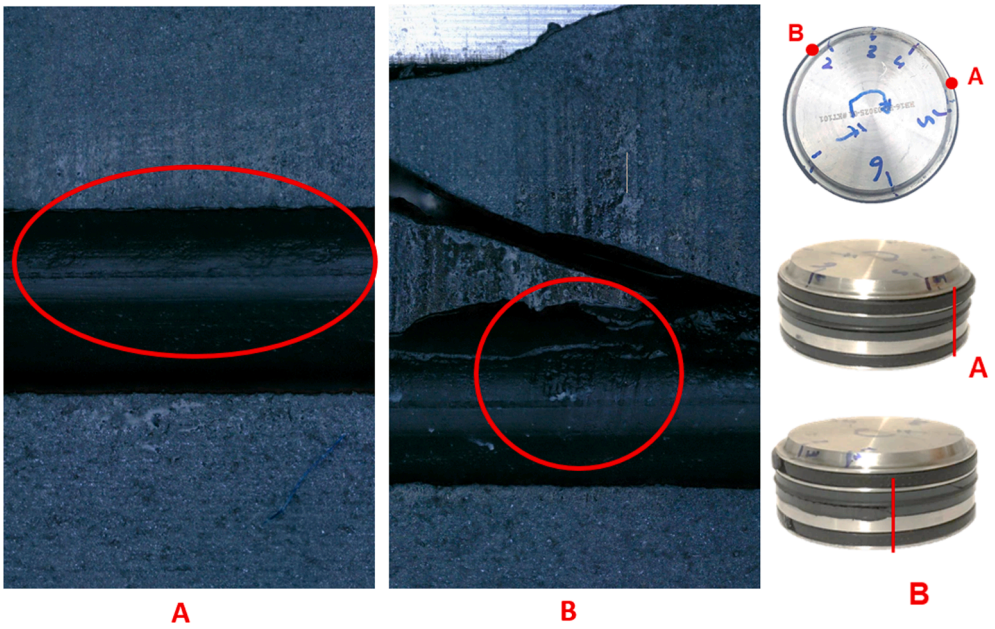


Fig. 14. Pre-Extrusion elastomer nibbled extrusion.

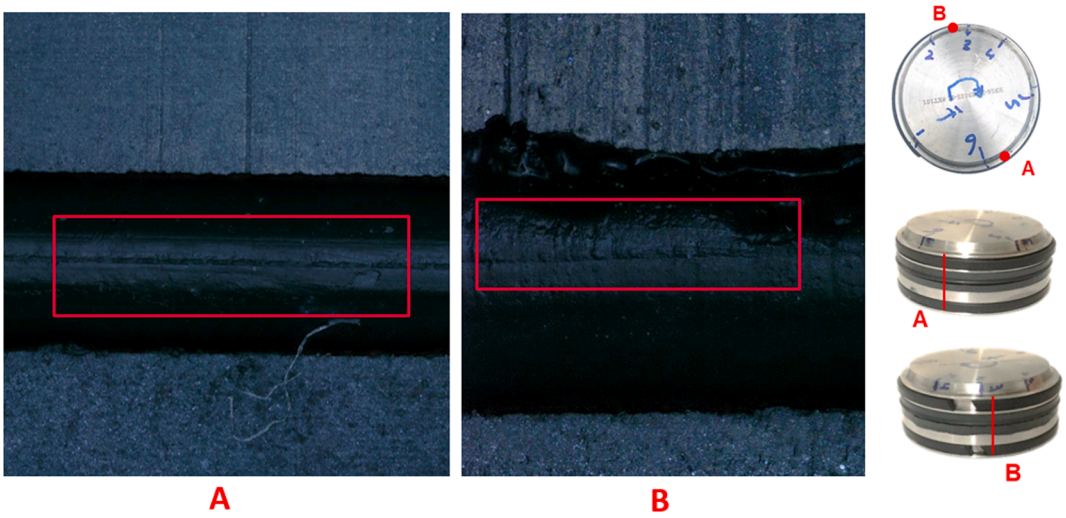


Fig. 15. Pre-extrusion elastomer thermal degradation.

The accumulation of nibbled extrusion and thermal degradation cause significant loss of sealing performance. When that damage corresponds to the cut in the PTFE back-up ring, the fluid is allowed to fill the gap and radially strain it (Fig. 16). The low-pressure backup ring is then pushed onto the damper body. Fig. 17 shows the low radial stiffness of the back-up as two fingers alone provide sufficient force to bend it outward.

The radial deformation of the back-up rings leads to the thinnening of the oil film with a rapid increase in friction and the PTFE is then extruded through the operating clearance between the piston and the damper body. Vertical wear marks from section 3 shown in Fig. 18, support lack of lubrication as the cause of extrusion. Discoloration and the prevelance of plastic flow rather than cracking also suggests that high temperature rather than high oil pressure is the main contributor to the extrusion. This was also confirmed when a cross-section of the extruded portion showed no signs of cracks under the microscope.

The increased gap due to the extrusion allows the oil under pressure to push and roll the seal out of its seat causing excessive wear (Fig. 19). This is observed in several locations three of them, namely A, B and C, are shown in Fig. 19.

The unseating of the elastomer reduces the available system clearance forcing metal on metal contact between the piston and the damper body. The metal-to-metal contact causes wear marks on the external surface of the piston that slides with friction on the internal surface of the cylinder producing the marks shown in Fig. 20. Similarly, wear marks were found on the sealing surface of the



Fig. 16. Fluid flow through back-up ring gap.

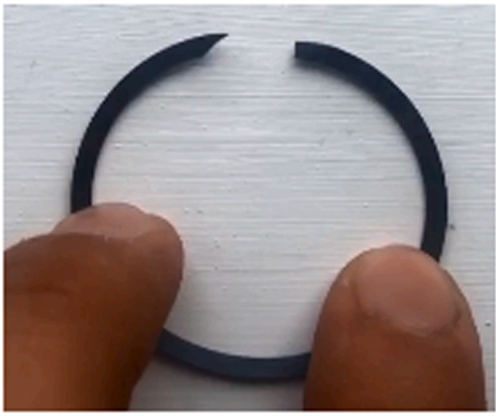


Fig. 17. Back-up ring low radial stiffness.

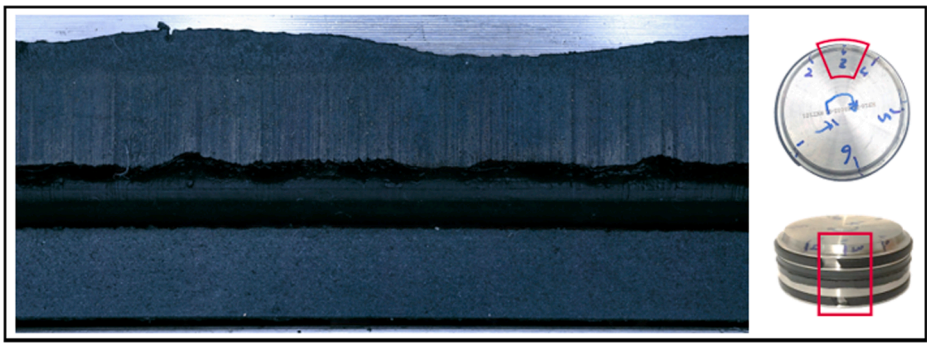


Fig. 18. Section 3 PTFE extrusion.

damper body.

The seal failure consists of the accumulation of damage on the elastomer followed by a loss of sealing performance. Seal damages in sections without back-up ring extrusion proved that the elastomer damage is the first to appear. The damage aligned with the back-up ring cut allows the system fluid pressure to radially deform and extrude the back-up ring through the clearance. Without the support of the back-up ring, the elastomer is pushed and rolled out of its seat and metal to metal contact wear occurs between the piston and body.

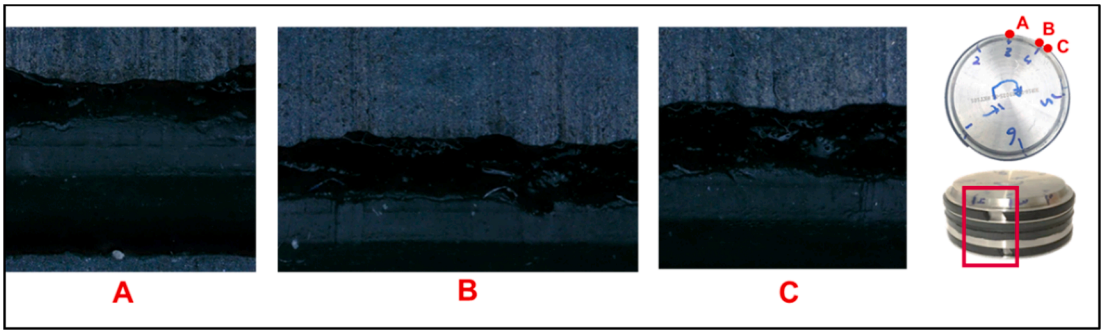


Fig. 19. Unseating damage to the elastomer.

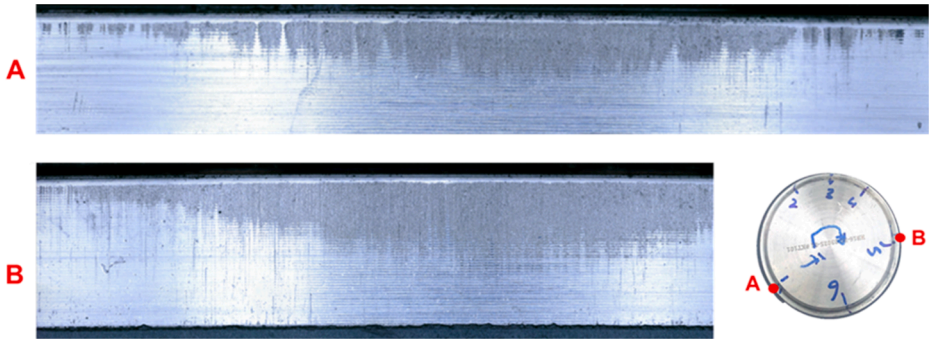


Fig. 20. Piston damage.

4. Material characterisation

For the PTFE material a polynomial model with three terms was chosen and is shown in Fig. 21. On the other hand, the best fitting model for the Fluorocarbon material was a Mooney-Rivlin model with 3 terms (Fig. 22).

The thermal expansion coefficients were taken from literature and assumed to be 198 10^{-6}/K for the fluorocarbon [21] and 150 10^{-6}/K for the PTFE [22].

5. Simulation

The cut in the back-up was identified as a key component in the failure of the sealing system and the FE model needed to incorporate this feature to capture its effects on the stress and strain field. The model described in section 3 was used to carry out the multistep analysis considering interference fit, thermal analysis and estimate the deformation of the seal under the oil pressure. Results from the interference fit simulation show a maximum stress level of 14.2 MPa and 11.9 MPa in the body and piston, respectively (see Fig. 23). The low stress level in the metallic parts is to be expected as the interference is mostly compensated by the deformation of the seal due to significantly lower modulus of elasticity of the elastomer. The sealing pack is interested by a significantly lower stress with the maximum located beneath the contact surface as expected considering the Hertzian contact theory (Fig. 24).

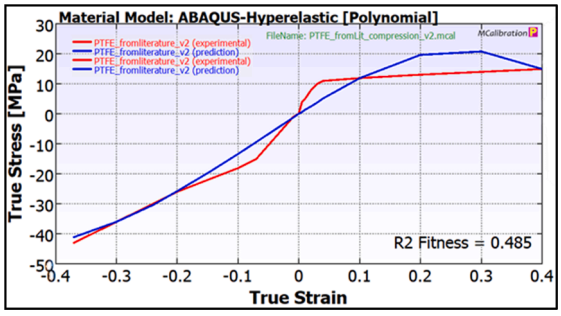


Fig. 21. PTFE stress–strain curve fitted with a hyperelastic polynomial model.

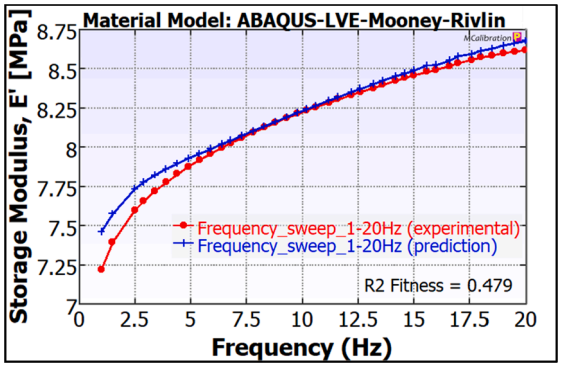


Fig. 22. Fluorocarbon DMA Data fitted with Mooney-Rivlin Model.

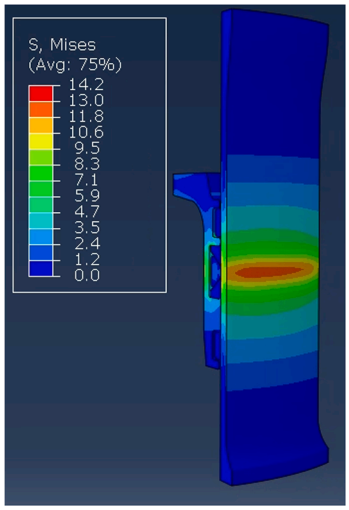


Fig. 23. Interference fit stress levels.

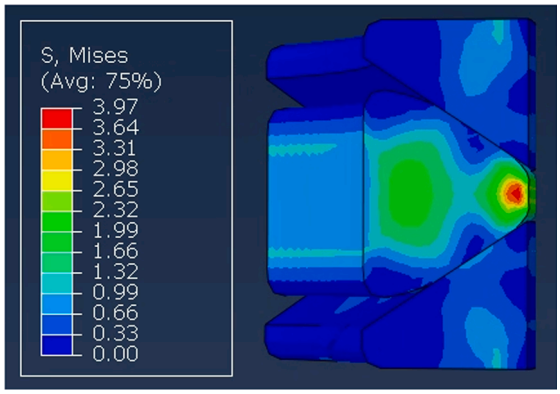


Fig. 24. Interference fit: seal pack stress levels.

A notable finding is that higher levels of stress are experienced on the elastomer along the line of the low-pressure back-up ring cut as seen in (Fig. 25). Moreover, stress concentration is observed along the edges of the cut back-up ring (see Fig. 26).

This corresponds to a higher maximum stress in the low-pressure back-up ring compared to the high-pressure back-up ring at 4.51 MPa (Fig. 27) and 2.25 MPa (Fig. 28) respectively.

The results of the thermal analysis show as expected minimum variation in the stress with the maximum equal to 3.93 MPa (Fig. 29) against the value of 3.97 MPa attained at the end of the interference fit analysis. This is mostly due to the small difference in the

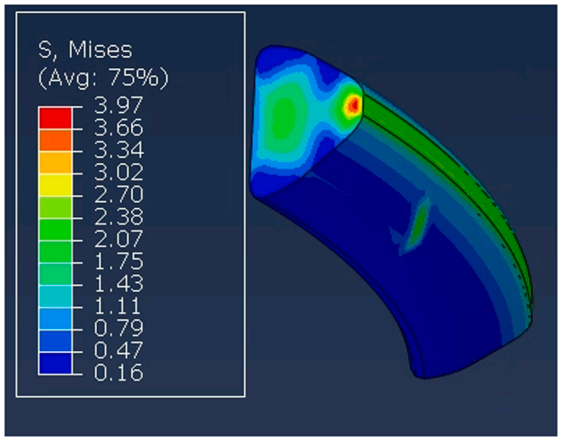


Fig. 25. Elastomer stress levels.

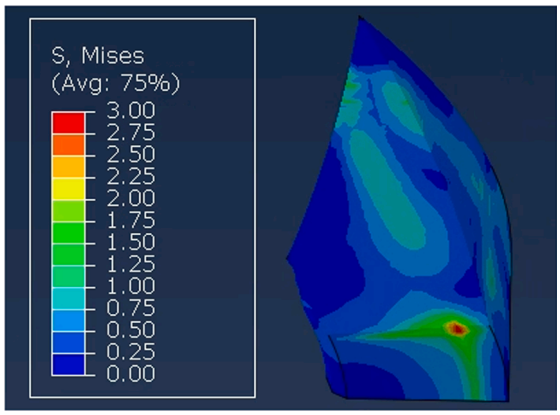


Fig. 26. Low-pressure back-up ring.

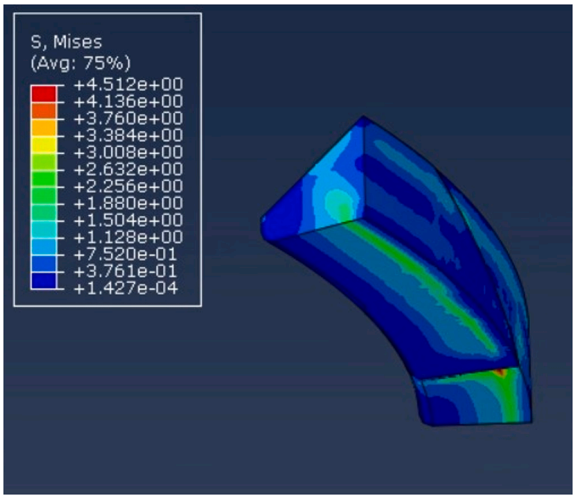


Fig. 27. Interference fit stress levels.

coefficient of thermal expansion used for the seal compared to the steel parts. Higher stress along the low-pressure back-up ring cut is also observed with an increase in the maximum stress to 4.71 MPa (Fig. 30) due to the thermal expansion of the back-up rings and the piston surrounding the sealing pack that restrains the free expansion of the seal in the radial and axial direction.

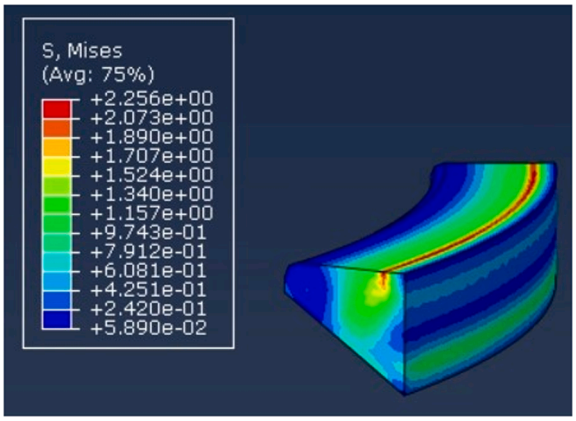


Fig. 28. Interference fit: seal pack stress levels.

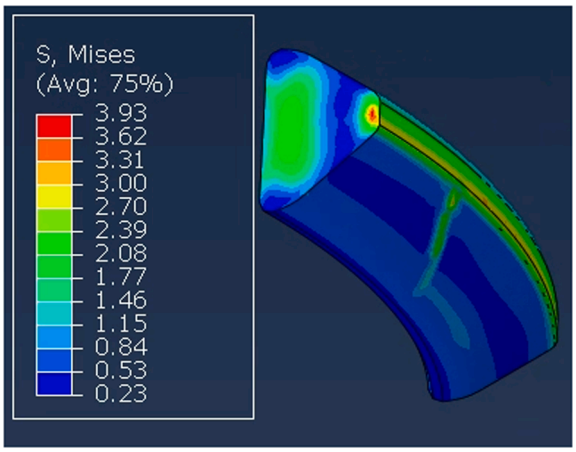


Fig. 29. Temperature step: elastomer stress levels.

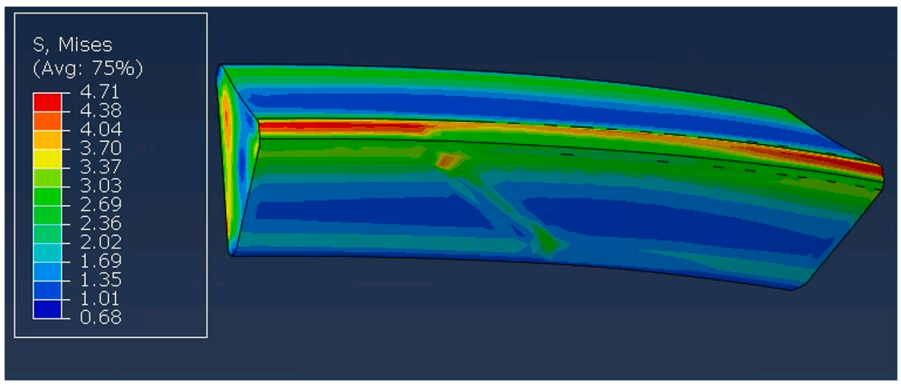


Fig. 30. Pressure step: elastomer stress levels.

After the pressure step, the stress increases mostly at the tip of the back-up ring cut and it decreases at the coincident elastomer surface (Fig. 32). The contact pressure distribution also shows an increase in the maximum stress value in correspondence of the back-up ring cut (Fig. 31).

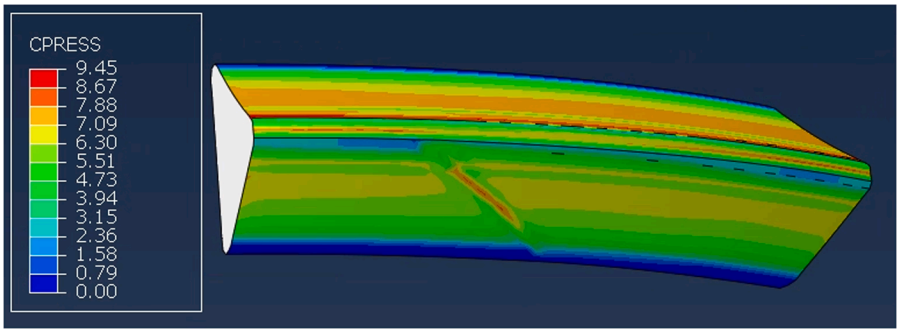


Fig. 31. Pressure step: elastomer contact stress.

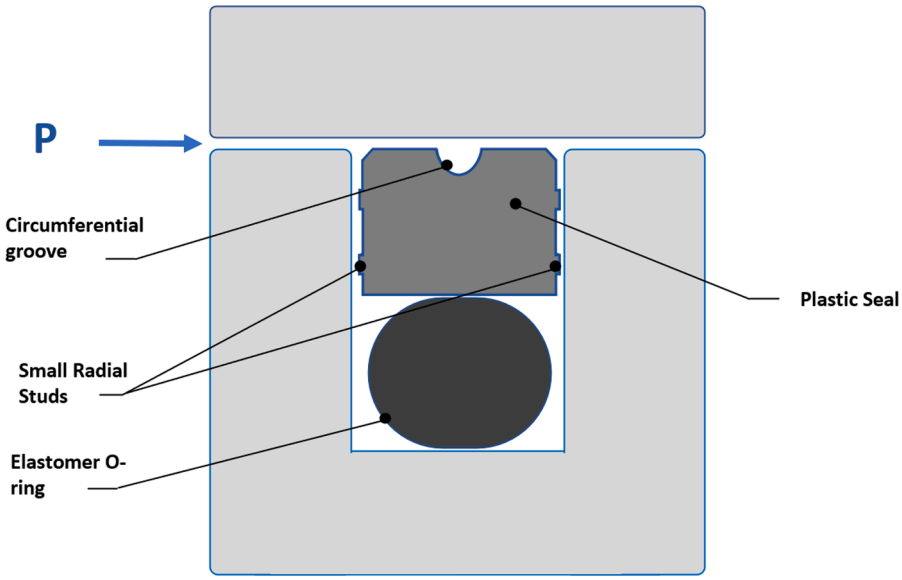


Fig. 32. Suitable seal example.

6. Discussion

Three key information on the onset and evolution of the seal damage are identified from the failure analysis. The failure mechanisms, their sequence and the operating condition during failure are established as a result of the combined experimental and numerical approach.

Table 1 summarises the observed failure mechanisms and their possible causes. A common cause for failure in four of the five failure mechanisms is exposure to high heat which is typically caused by excessive contact pressure or friction.

The failure has been observed in service at pressures below maximum, temperatures within the seal's operating window and under conditions within the normal range of operation.

The chosen seal is designed for long strokes and low frequency applications wherein a full lubricating film would be able to form. However, in its current application it could also experience high frequencies and short strokes.

Results from simulations highlight that the region surrounding the back-up ring cut contributes to seal failure. von Mises stress and

Table 1
List of observed failure mechanisms and possible causes.

Damage	Possible Causes
Elastomer Nibbled extrusion	Excessive pressure, excessive friction
Elastomer Thermal degradation	Excessive temperature
PTFE Wear Marks	High Pressure, Insufficient lubrication, Incorrect counter-surface temperature
PTFE Discolouration	Excessive temperature
PTFE plastic flow extrusion	Excessive temperature

contact pressures experienced during the press-fit are well below the seal's maximum operating pressure of 35 MPa. This confirms that induced contact pressures during the press-fitting stage are within reasonable levels and are highly unlikely to be a contributing factor to seal failure.

Furthermore, stress results after each step highlighted the line along the back-up ring cut as a region of higher stress for the elastomer. This becomes even more apparent when the internal oil pressure is applied, as a more concentrated stress develops at the tip of the cut line along with reduced contact pressure at the seal contact surface. The back-up ring cut is a significant contributor to seal failure, especially considering that the high stress region appears at pressures significantly lower than those under operating condition. The peak stress suggests that the region is likely to experience damage while the reduced contact pressure on the surface suggests potentially higher local leakage.

The failure analysis suggests that the accumulation of elastomer damage is a result of insufficient lubrication during high frequency short stroke applications. Insufficient lubrication combined with high contact pressure produces the oil film to break resulting in an increase of friction and temperature at the elastomer sealing face where the higher friction coefficient of the elastomer makes it more dependent on lubrication. This would explain why damage occurs on the elastomer first. Moreover, the damage condition paired with accumulated rather than instantaneous damage would explain why the seal is failing at inconsistent operating conditions. This was further supported through the results of the simulations which excluded high initial pressures from press-fit and highlighted the back-up ring cut as an instrumental part of the failure because responsible of stress concentration.

Ultimately, the cause of seal failure goes back to a seal design that does not satisfy the full range of operating condition of a high-performance racing car. Reliability, of the seal, and damper could be significantly improved by choosing a more appropriate seal design with specific features that ensure sufficient lubrication at high frequency, low amplitude oscillations.

7. Alternative seal design

A more suitable design would consist of an elastomer seal with notches or studs along the sides of the seal to prevent blow-by [9] as well as a groove along the circumference to retain the oil and ensure consistent lubrication. In addition, sloping sides with a positive gradient can be incorporated to promote fluid flow into the circumferential groove. By using PTFE material at the dynamic sealing surface between the seal pack and the body, friction is further reduced by eliminating stick–slip while the material's wider temperature range makes the seal more resistant to increased temperature in the case of dry running. Fig. 29 shows an example of a suitable seal displaying the above-mentioned features.

Conclusions

Using a combined numerical and experimental approach the failure analysis of a damper hydraulic seal for racing cars has been investigated. From the evidence gathered by means of direct observation of the seal and the numerical modelling of its service conditions the following conclusions can be drawn:

a. The failure sequence has been reconstructed identifying an accumulation of elastomer damage in correspondence of the back-up ring cut with extrusion of this latter through the gap and, finally, the unseating of the elastomer.
b. The FE model was used to simulate press-fitting and operational conditions of temperature and pressure. These results showed an increase in stress on the elastomer along the back-up ring cut thus highlighting the region as sensitive to increased levels of elastomeric damage and supporting the failure sequence.
c. The deduced root cause of the seal's failure was identified as the accumulation of elastomer damage because of insufficient lubrication during high frequency, short stroke applications. An alternative design is identified to overcome the failure analysed.

Declaration of Competing Interest

The authors declare that they have no known competing financial interests or personal relationships that could have appeared to influence the work reported in this paper.

References

[1] G.K. Nikas, Eighty years of research on hydraulic reciprocating seals: review of tribological studies and related topics since the 1930s, Proc. Inst. Mech. Eng. Part J J. Eng. Tribol. 224 (1) (2010) 1–23.
[2] C.M. White, D.F. Denny, The sealing mechanism of flexible packings, HM Stationery Office London (1972).
[3] K. Yoshimura, N. Suzuki, H. Mizuta, Oil film formation of reciprocating seals observed by interferometry, Tribol. Online 9 (3) (2014) 106–112.
[4] F. Hirano, M. Kaneta, Theoretical investigation of friction and sealing characteristics of flexible seals for reciprocating motion, in: Proceedings of 5th International Conference on Fluid Sealing, 1971, pp. G2–G17.
[5] S. Bhaumik, A. Kumaraswamy, S. Guruprasad, P. Bhandari, Study of effect of seal profile on tribological characteristics of reciprocating hydraulic seals, Tribol. Ind. 37 (2) (2015) 264.
[6] A.S. Rana, R.S. Sayles, An experimental study on the friction behaviour of aircraft hydraulic actuator elastomeric reciprocating seals vol. 48 (2005) 507–515.
[7] G. Cheng, F. Guo, X. Zang, Z. Zhang, X. Jia, X. Yan, Failure analysis and improvement measures of airplane actuator seals, Eng. Fail. Anal. 133 (2022), 105949.
[8] Y. Zhang, J. Shi, S. Wang, C. Zhang, M.M. Tomovic, Sealing mechanism and failure analysis of actuator reciprocating seal, in: 2016 IEEE 11th Conference on Industrial Electronics and Applications (ICIEA), 2016, pp. 2190–2195.
[9] S. Xu, Z. Su, J. Wu, Analysis on sealing performance of VL seals based on mixed lubrication theory, Ind. Lubr. Tribol. 71 (1) (2019) 54–60.
[10] G.K. Nikas, Theoretical study of solid back-up rings for elastomeric seals in hydraulic actuators, Tribol. Int. 37 (9) (2004) 689–699.

[11] G.K. Nikas, Elastohydrodynamics and mechanics of rectangular elastomeric seals for reciprocating piston rods, J. Trib. 125 (1) (2003) 60–69.
[12] G.K. Nikas, Analytical study of the extrusion of rectangular elastomeric seals for linear hydraulic actuators, Proc. Inst. Mech. Eng. Part J J. Eng. Tribol. 217 (5) (2003) 365–373.
[13] G.K. Nikas, Transient elastohydrodynamic lubrication of rectangular elastomeric seals for linear hydraulic actuators, Proc. Inst. Mech. Eng. Part J J. Eng. Tribol. 217 (6) (2003) 461–473.
[14] R.F. Salant, N. Maser, B. Yang, Numerical model of a reciprocating hydraulic rod seal, International Joint Tribology Conference 42592 (2006) 577–583.
[15] R.K. Flitney, Seals and sealing handbook, Elsevier, 2011.
[16] Trelleborg, "Hydraulic seals – linear," *Solutions*, p. 262, 2011.
[17] W. Li, S. Mays, D. Lam, Material and finite element analysis of poly (tetrafluoroethylene) rotary seals, Plast. rubber Compos. 31 (8) (2002) 359–363.
[18] A.S.U. Manual, "Abaqus 6.11," http://130.149, vol. 89, no. 2080, p. v6, 2012.
[19] J. Qu, P.J. Blau, T.R. Watkins, O.B. Cavin, N.S. Kulkarni, Friction and wear of titanium alloys sliding against metal, polymer, and ceramic counterfaces, Wear 258 (9) (2005) 1348–1356.
[20] R. Keresztes, L. Zsidai, G. Kalácska, P. De Baets, Friction of polymer/steel gear pairs, Sci. Bull. Ser. C Fascicle Mech. Tribol. Mach. Manuf. Technol. 23 (63) (2009) 2009.
[21] G.P. Rutledge, Correlation of critical temperatures with thermal expansion coefficients of liquid fluorocarbons, Carbide and Carbon Chemicals Corp, Oak Ridge, TN (USA), 1949.
[22] L. Holliday, J. Robinson, The thermal expansion of composites based on polymers, J. Mater. Sci. 8 (3) (1973) 301–311.



https://dspace.org/

Experimental and numerical investigation of heave damper hydraulic seal for racing car

Azar, Michel; Grasso, Marzio; Rose, Timothy; Carless, Owen; St Leger-Harris, Chris ...

2022-06-29
Elsevier
https://doi.org/10.1016/j.engfailanal.2022.106557
Azar M, Grasso M, Rose T, et al., (2022) Experimental and numerical investigation of heave damper hydraulic seal for racing car. Engineering Failure Analysis, Volume 140, October 2022, Article number 106557

Downloaded from a DSpace repository. https://dspace.org/